NANO LETTERS

pubs.acs.org/NanoLett

Letter

Photothermal Attenuation of Cancer Cell Stemness, Chemoresistance, and Migration Using CD44-Targeted MoS_2 Nanosheets

Jinyuan Liu, Steve Smith, and Congzhou Wang*

Cite This: *Nano Lett.* 2023, 23, 1989−1999

Read Online

ACCESS | Metrics & More | Article Recommendations | Supporting Information

ABSTRACT: Cancer stem-like cells (CSCs) play key roles in chemoresistance, tumor metastasis, and clinical relapse. However, current CSC inhibitors lack specificity, efficacy, and applicability to different cancers. Herein, we introduce a nanomaterial-based approach to photothermally induce the differentiation of CSCs, termed "photothermal differentiation", leading to the attenuation of cancer cell stemness, chemoresistance, and metastasis. MoS_2 nanosheets and a moderate photothermal treatment were applied to target a CSC surface receptor (i.e., CD44) and modulate its downstream signaling pathway. This treatment forces the more stem-like cancer cells to lose the mesenchymal phenotype and adopt an epithelial, less stem-like state, which shows attenuated self-renewal capacity, more response to anticancer drugs, and less invasiveness. This approach could be applicable to various cancers due to the broad availability of the CD44 biomarker. The concept of using photothermal nanomaterials to regulate specific cellular activities driving the differentiation of CSCs offers a new avenue for treating refractory cancers.

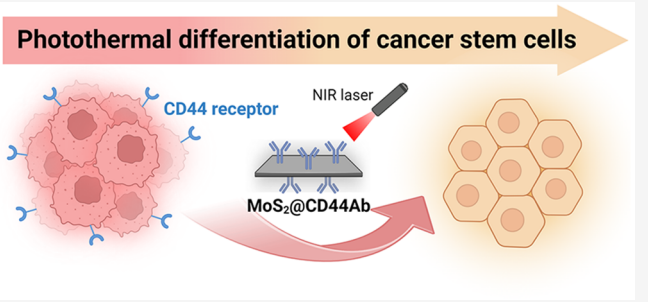

KEYWORDS: *MoS_2 nanosheets, CD44, photothermal differentiation, cancer cell stemness, chemoresistance*

Chemoresistance, metastasis, and recurrence pose major challenges in cancer therapy.[1,2] Cancer stem-like cells (CSCs) are responsible for these challenges owing to their self-renewal property, aggressive invasiveness, and ability to resist chemotherapeutic drugs.[3,4] To date, two major routes have been taken to tackle CSCs. The first route is to develop agents that exert preferential cytotoxicity toward CSCs.[5,6] Despite its promise, nonspecificity and inadequate understanding of the CSC-specific apoptotic pathway remain the main obstacles.[7] More importantly, non-CSCs can spontaneously gain stemness and transform into CSCs, further reducing the effectiveness of this approach.[8−10] The second route, termed the "differentiation strategy", has recently received substantial attention, as it converts CSCs from a dedifferentiated, high-stemness state to a differentiated, low-stemness state by using small molecules such as second messengers and retinoic acid.[11−13] Such induced differentiation places cancer cells in a less stem-like state, where they show more sensitivity to anticancer drugs.[14,15] However, this strategy also suffers from nonspecificity and requires the sophisticated design of a targeted delivery system, along with the limited efficacy and applicability to different cancers.[11,16] To this end, a refined "differentiation strategy" with high specificity to CSCs and broad applicability to various cancers is greatly needed.

CD44, a transmembrane adhesion receptor, is recognized as a key biomarker for CSCs.[17] It is highly expressed on breast,[18] prostate,[19] ovarian,[20] pancreatic,[21] colon,[22] and liver cancers.[23] Clinical data show that a high level of CD44 correlates to a poor prognosis for patients.[24] It was found that CD44 induces a phenotypic change in cancer cells, a cellular process named an epithelial−mesenchymal transition (EMT), during which cancer cells lose the original epithelial phenotype and acquire a mesenchymal phenotype with enhanced stemness, chemoresistance, and invasiveness.[25] Conversely, knock-down of CD44 attenuates the mesenchymal phenotype, slows cancer progression, and weakens therapeutic resistance.[26,27] Therefore, CD44 is a promising therapeutic target to attenuate cancer stemness, chemoresistance, and metastasis.[28,29] However, existing efforts have so far mostly utilized CD44 as a surface receptor for targeting CSCs, for instance, using hyaluronan-functionalized nanodelivery systems to target CSCs,[12,13] while the functional roles of CD44 in gaining mesenchymal phenotype and maintaining cancer stemness have not been fully exploited.

Received: January 7, 2023
Revised: February 18, 2023
Published: February 24, 2023

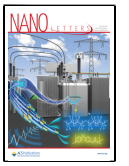

https://doi.org/10.1021/acs.nanolett.3c00089
Nano Lett. 2023, 23, 1989−1999

Scheme 1. Concept of "Photothermal Differentiation" of Cancer Stem Cells Using CD44-Targeted MoS_2 Nanosheets to Attenuate Cancer Cell Stemness, Drug Resistance, and Invasiveness[a]

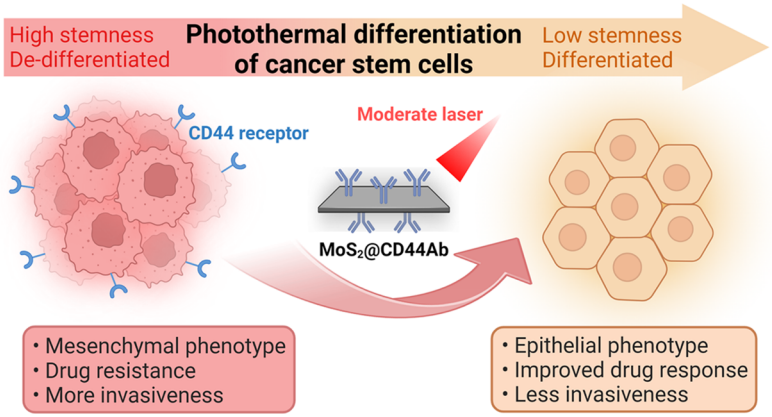

[a]Unlike conventional photothermal therapy, this approach applies a moderate photothermal effect to modulate CD44-regulated signaling activities and convert mesenchymal/stem-like cancer cells to an epithelial/less stem-like phenotype.

Here, we present a nanomaterial-based approach using CD44-targeted MoS_2 nanosheets to photothermally attenuate cancer stemness by modulating CD44-regulated signaling activities and converting mesenchymal/stem-like cancer cells to an epithelial/less stem-like phenotype. Unlike conventional photothermal therapy in which cancer cells are ablated by elevated local temperature,[30−36] this approach applies a moderate photothermal effect (43 °C) to modulate specific cellular activities involving the differentiation of CSCs. We coin this approach "photothermal differentiation" (Scheme 1). MoS_2 nanosheets are chosen as photothermal nanotransducers owing to their excellent biocompatibility, photothermal conversion efficacy, and ease of surface functionalization.[37−41] We demonstrate the feasibility of this approach on triple-negative breast cancer and malignant prostate cancer cell lines; both cells are CD44-overexpressed, are enriched with features associated with stem-like/mesenchymal phenotypes, and have the worst prognosis.[42,43] By driving the phenotypic change and differentiation of CSCs, this approach attenuates cancer cell stemness, drug resistance, and migration/invasion. Importantly, the molecular mechanism by which this approach drives the phenotypic transition and stemness attenuation is determined.

MoS_2 nanosheets were prepared using a liquid exfoliation method.[44] To endow the nanosheets with CD44-targeting ability, the surface of nanosheets was first coated with a layer of protein A (PA) mixed with bovine serum albumin (BSA) (i.e., MoS_2@PA) via strong hydrophobic interactions,[45] followed by a subsequent conjugation with CD44 antibodies (i.e., MoS_2@PA@CD44Ab) (Figure 1A). Here, each PA molecule contains several binding sites for the Fc domain of antibodies, ensuring the optimal orientation of surface antibodies with Fab domains facing outward,[46] whereas BSA serves as a spacer to control the density of PA and antibodies on the nanosheet surface, preventing the steric crowding of Fab domains from neighboring antibodies.[47]

Transmission electron microscopy (TEM) showed that the lateral dimensions of as-synthesized MoS_2@PA@CD44Ab are 162.4 ± 33.5 nm in length and 103.1 ± 21.9 nm in width (Figure 1B and Figure S1), whereas the pristine MoS_2 nanosheets have a smaller lateral size (Figure S2). Atomic force microscopy (AFM) indicated a progressive increase in the thickness of MoS_2 nanosheets following each step of functionalization (Figure 1C): bare MoS_2 (5 nm), MoS_2@PA (8 nm), and MoS_2@PA@CD44Ab (13 nm). The successful functionalization was further evident from the increased hydrodynamic size of the nanosheets (increasing from 137.4 to 147.1 and 165.3 nm, Figure 1D) and gradually elevated ζ potential (Figure 1E). The excellent coating and colloidal stability of MoS_2@PA@CD44Ab were manifested by the negligible change in the hydrodynamic size when it was dispersed in different media for 1 week (Figure S3). The absorbance spectrum of MoS_2@PA@CD44Ab covers the near-infrared region, making it an effective photothermal agent (Figure S4). As shown in Figure 1F, after 5 min exposure under an 808 nm laser (0.35 W/cm^2), the aqueous solution dispersed with 200 μg/mL MoS_2@PA@CD44Ab elevated its temperature from 22 to 43 °C, whereas pure water only slightly increased its temperature. The photothermal stability of MoS_2@PA@CD44Ab nanosheets was further validated by monitoring the temperature of a nanosheet suspension during several laser ON/OFF cycles, while the temperature profile of the nanosheet suspension did not exhibit an observable change (Figure 1G). These results suggest the successful preparation of CD44-targeted MoS_2 nanosheets, hereafter referred to as MoS_2@CD44Ab.

To track and quantify the cell uptake of MoS_2 nanosheets, a triple-negative breast cancer cell line (i.e., MDA-MB-231) with a relatively higher degree of stemness, invasiveness, and CD44 expression was selected.[48] The abundance of cell surface CD44 was validated by immunofluorescence imaging (Figure S5). An equal amount of FITC-BSA was coated onto the surface of nanosheets when preparing the nontargeted MoS_2@BSA and CD44-targeted MoS_2 (i.e., MoS_2@CD44Ab). As shown in Figure 1H and Figure S6, compared to untreated cells and cells incubated with nontargeted MoS_2@BSA, MDA-MB-231 cells incubated with MoS_2@CD44Ab displayed higher fluorescence intensity, suggesting the surface functionalization of theCD44 antibody facilitated the cell uptake of nanosheets. This was further reinforced through a receptor-blocking experiment. It was found that most cell-internalized nanosheets were entrapped in the lysosomal degradative compartments, as manifested by the fluorescence overlap between the nanosheets and Lysotracker dye (Figure 1I and Figure S7). The biocompatibility of MoS_2 nanosheets and laser treatment were evaluated through a panel of cytotoxicity assays (Figure

https://doi.org/10.1021/acs.nanolett.3c00089
Nano Lett. 2023, 23, 1989−1999

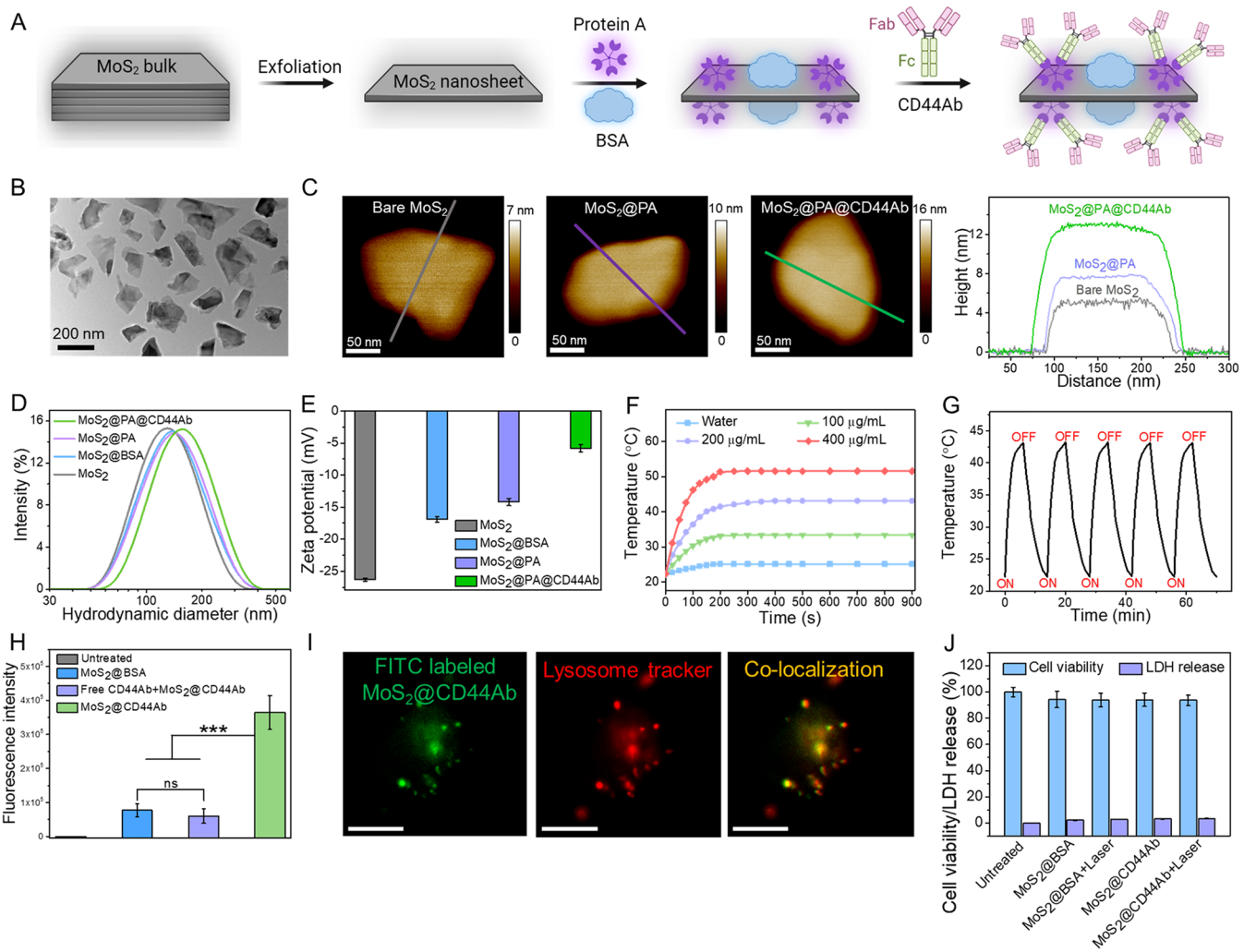

Figure 1. Preparation and characterization of CD44-targeted MoS_2 nanosheets. (A) Steps used for preparing CD44-antibody-functionalized MoS_2 nanosheets. (B) Transmission electron microscopy image of MoS_2@PA@CD44Ab. (C) Atomic force microscopy thickness measurement of MoS_2 nanosheets after every step of surface functionalization. (D, E) Dynamic light scattering and ζ potential of MoS_2, MoS_2@BSA, MoS_2@PA, and MoS_2@PA@CD44Ab. Error bars: SD, n = 5. (F) Temperature of an MoS_2@PA@CD44Ab suspension excited by an 808 nm laser. (G) Temperature of a MoS_2@PA@CD44Ab suspension (200 μg/mL) over five times of ON/OFF laser irradiation cycles. (H) Fluorescence images of MDA-MB-231 cells incubated with FITC-labeled MoS_2 nanosheets. Error bars: SD, n = 20. One-way ANOVA, ns = no significant difference, ***P < 0.001. (I) Intracellular localization of FITC-labeled MoS_2 nanosheets in MDA-MB-231 cells. Scale bars: 20 μm. (J) Cell viability and lactate dehydrogenase (LDH) assays of MDA-MB-231 cells following different treatments. Error bars: SD, n = 5.

1J and S8). Together, these assays suggest negligible cytotoxicity of MoS_2 nanosheets and laser treatment at the selected doses, which set the stage for the evaluation of their influence on the cancer cell stemness, drug resistance, and migration.

In cancer cells, the ability to form mammospheres has been used as a measure of cancer cell stemness and self-renewal capacity, which dictates the tumor-regenerative potential.[49,50] Therefore, mammosphere formation assays were utilized to investigate the effect of MoS_2@CD44Ab and the moderate laser treatment on the stemness-high MDA-MB-231 cells. Prior to treatment, MDA-MB-231 cells were cultivated to either adherent monolayers (i.e., 2D-cultured model) or mammospheres (i.e., 3D-cultured model intended to enrich CSCs) (Figure 2A). The cells after different treatments were collected and seeded into ultralow-attachment plates to observe the mammosphere formation. For the untreated cells, both 2D- and 3D-cultured cells formed significant amounts of mammospheres after 7 days of culture under the suspension condition, while the 3D-cultured cells led to a larger size and number of mammospheres due to the enrichment of CSCs.[51] MoS_2@BSA and MoS_2@BSA+Laser treatments did not significantly change the mammosphere-forming ability. Importantly, MoS_2@CD44Ab diminished the number and size of mammospheres for both 2D- and 3D-cultured cells, while MoS_2@CD44Ab+Laser further reduced the number and size of mammospheres to a minimal level (Figure 2B and Figures S9 and S10). A quantitative analysis indicates that MoS_2@CD44Ab+Laser treatment almost eliminated the larger-sized mammospheres (>150 μm) and decreased the number of smaller-sized mammospheres (70−150 μm) by more than 70% for both 2D- and 3D-cultured cell models (Figure 2C). At the molecular level, the expressions of cancer stemness markers Oct4, Sox2, and Nanog were evaluated by Western blotting. The results showed that MDA-MB-231 cells treated by MoS_2@CD44Ab reduced the expressions of Oct4, Sox2, and Nanog by 40−60%, whereas the cells treated by MoS_2@CD44Ab+Laser lowered the expres-

https://doi.org/10.1021/acs.nanolett.3c00089
Nano Lett. 2023, 23, 1989−1999

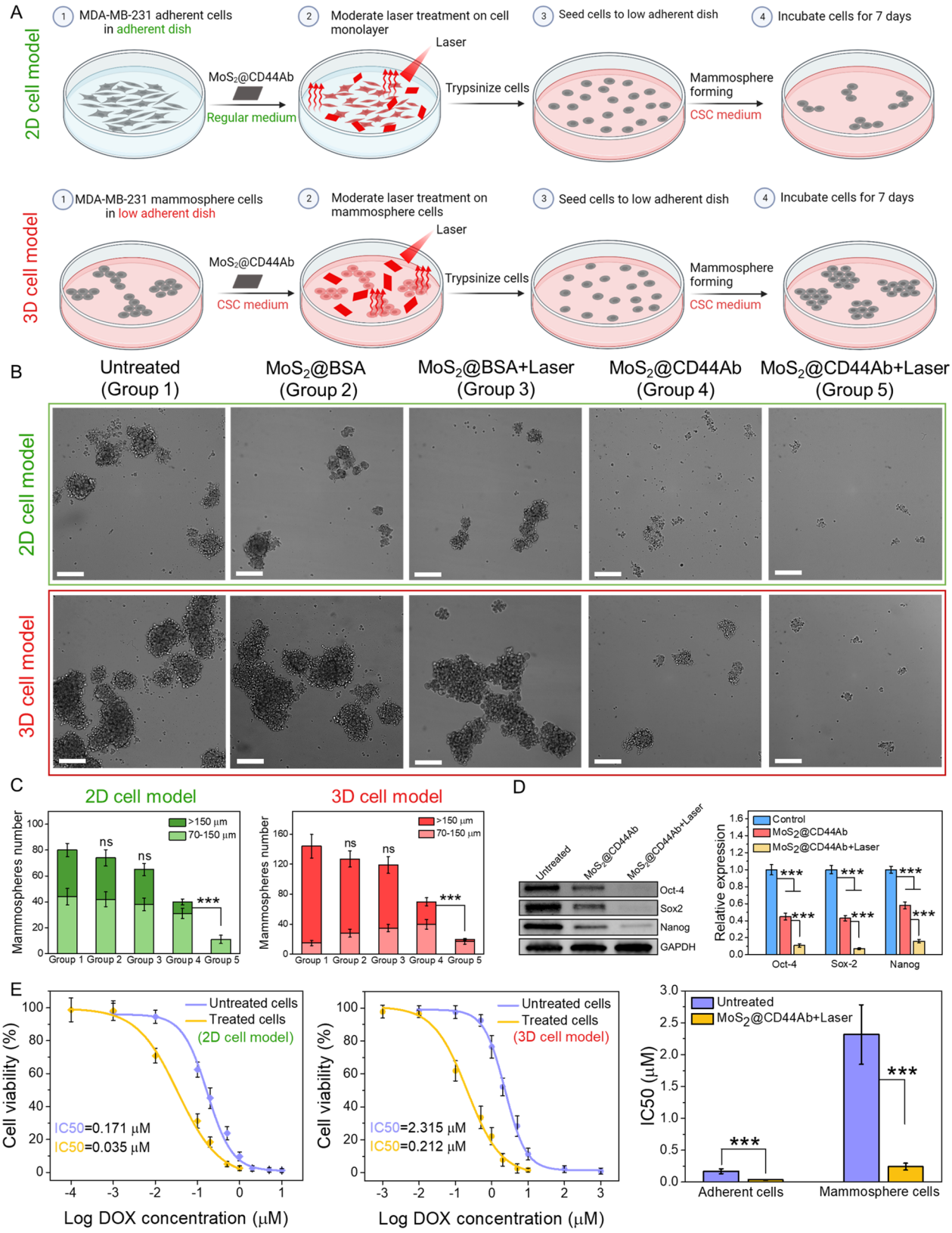

Figure 2. MoS_2@CD44Ab and laser treatment attenuate cancer cell stemness and drug resistance. (A) Schematic illustrating the process of conducting mammosphere formation assays using 2D-cultured and 3D-cultured cell models. (B) Mammosphere formation of MDA-MB-231 adherent and mammosphere cells subjected to various treatments. Scale bar: 200 μm. (C) Quantification of the mammospheres under 2D and 3D cell models (SD, n = 5). (D) Immunoblot analyses of stemness markers in MDA-MB-231 cells after treatment by MoS_2@CD44Ab and MoS_2@CD44Ab+Laser (SD, n = 3). (E) Dose-dependent cytotoxicity induced by DOX and IC_{50} values of DOX on MDA-MB-231 adherent and mammosphere cells with or without MoS_2@CD44Ab+Laser treatment (SD, n = 3). One-way ANOVA, ***$P < 0.001$.

https://doi.org/10.1021/acs.nanolett.3c00089
Nano Lett. 2023, 23, 1989−1999

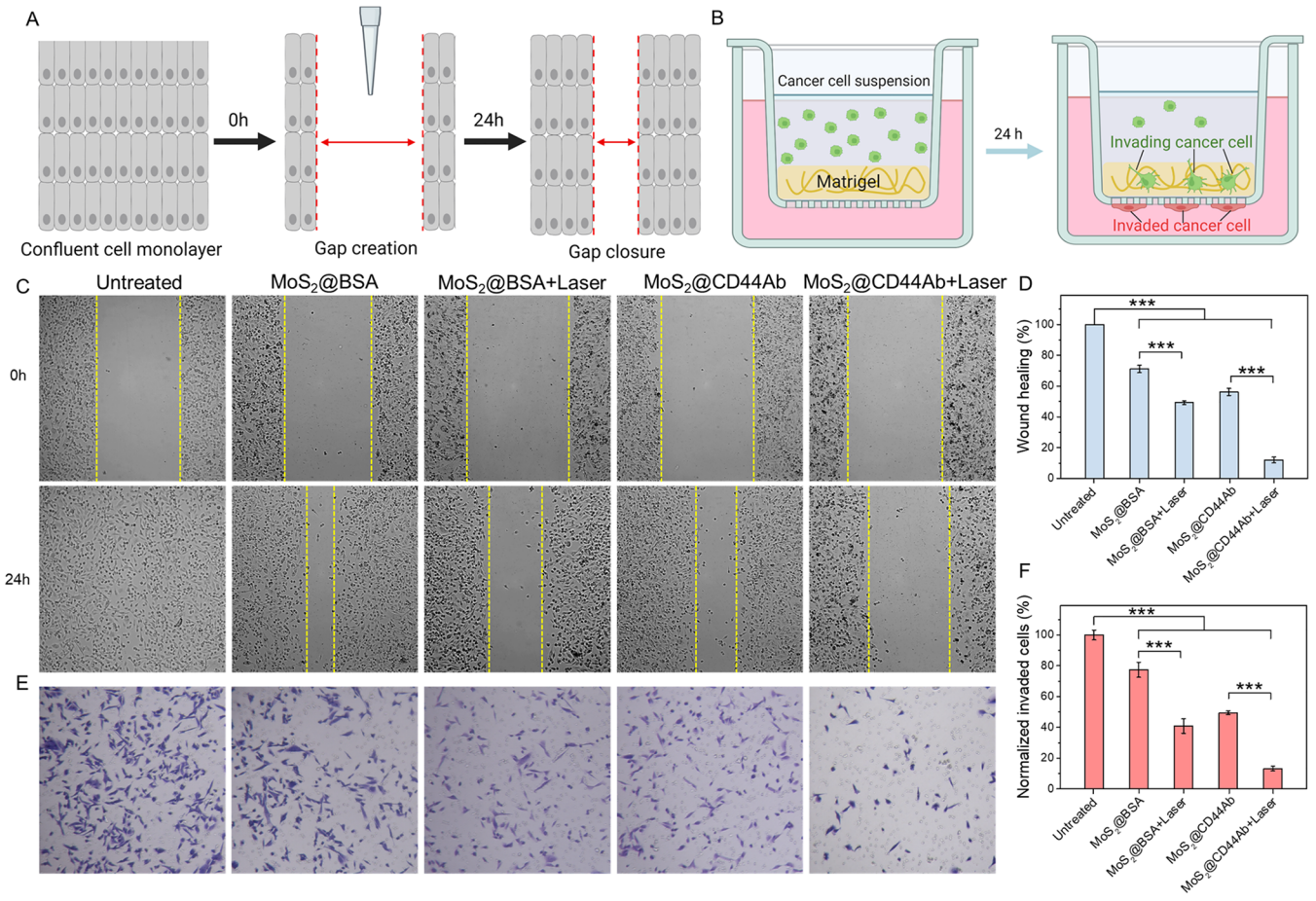

Figure 3. MoS_2@CD44Ab and laser treatment inhibit cancer cell migration and invasion. (A, B) Working principles of (A) wound-healing and (B) transwell invasion assays. (C, D) Percentage of gap closure in wound healing assays demonstrating that the migration ability of MDA-MB-231 cells was significantly impeded after treatment with MoS_2@CD44Ab+Laser. (E, F) Quantification of invaded MDA-MB-231 cells in transwell invasion assays demonstrating that the invasion ability of MDA-MB-231 cells was significantly impeded after treatment by MoS_2@CD44Ab+Laser. Error bars: SD, $n = 4$. One-way ANOVA, $***P < 0.001$.

sions of these markers by 80−90% (Figure 2D). These results demonstrate that MoS_2@CD44Ab and the moderate laser treatment synergistically attenuate the self-renewal capacity and stemness of MDA-MB-231 cells.

Apart from the self-renewal capacity, drug resistance is another important feature associated with cancer cell stemness.[52,53] Given that MoS_2@CD44Ab+Laser showed the best efficacy to attenuate stemness of MDA-MB-231 cells, the effect of this treatment on the response of cells to a traditional chemotherapeutic drug, doxorubicin (DOX), was investigated. Previous research showed that MDA-MB-231 cells possess intrinsic doxorubicin resistance due to their high stemness and mesenchymal phenotype.[54] 2D- and 3D-cultured MDA-MB-231 cells, with or without MoS_2@CD44Ab+Laser treatment, were subjected to a series of concentrations of DOX to identify the half-maximum inhibitory concentration (IC_{50}). As shown in Figure 2E, for the untreated cells, the 3D-cultured cells showed 13 times more resistance to DOX compared to the 2D-cultured cells (IC_{50}: 2.315 μM versus 0.171 μM), due to the enrichment of CSCs in the 3D-cultured model. However, after MoS_2@CD44Ab+Laser treatment, both 2D- and 3D-cultured cells displayed more sensitivity to DOX: the 2D-cultured adherent cells became 5 times as sensitive to killing by DOX (i.e., lower IC_{50} from 0.171 to 0.035 μM), while the 3D-cultured mammosphere cells became 10 times as sensitive to DOX (i.e., lower IC_{50} from 2.315 to 0.212 μM). These results suggest that MoS_2@CD44Ab and laser treatment can sensitize the intrinsically drug-resistant cancer cells to conventional anticancer drugs and potentially improve the therapeutic outcome of chemotherapy.

Molecular studies found that high CD44 expression correlates with tumor metastasis.[55,56] Therefore, the effect of MoS_2@CD44Ab and moderate laser treatment on the motility of MDA-MB-231 cells was assessed (Figure 3A,B). In the wound-healing assays, the percentage of gap closure within a given time window serves as an indicator of migration ability. For the untreated cells, we observed a complete gap closure (100%) within 24 h, indicating the potent migration ability of this cell line. The cells treated by MoS_2@BSA and MoS_2@BSA +Laser showed a modest gap closure. Remarkably, the cells treated by MoS_2@CD44Ab and MoS_2@CD44Ab+Laser displayed 60% and 10% gap closures, respectively (Figure 3C,D). Notably, the cells barely moved after being treated by MoS_2@CD44Ab+Laser, where the addition of laser irradiation following the MoS_2@CD44Ab treatment inhibited the cell migration to a higher extent, in comparison to treating cells with MoS_2@CD44Ab alone. As a control, a simple heating process by placing cells at 43 °C did not stop the cell migration (Figure S12). The same trend was present in the transwell invasion assays (Figure 3E,F), wherein only a few cells treated

https://doi.org/10.1021/acs.nanolett.3c00089
Nano Lett. 2023, 23, 1989−1999

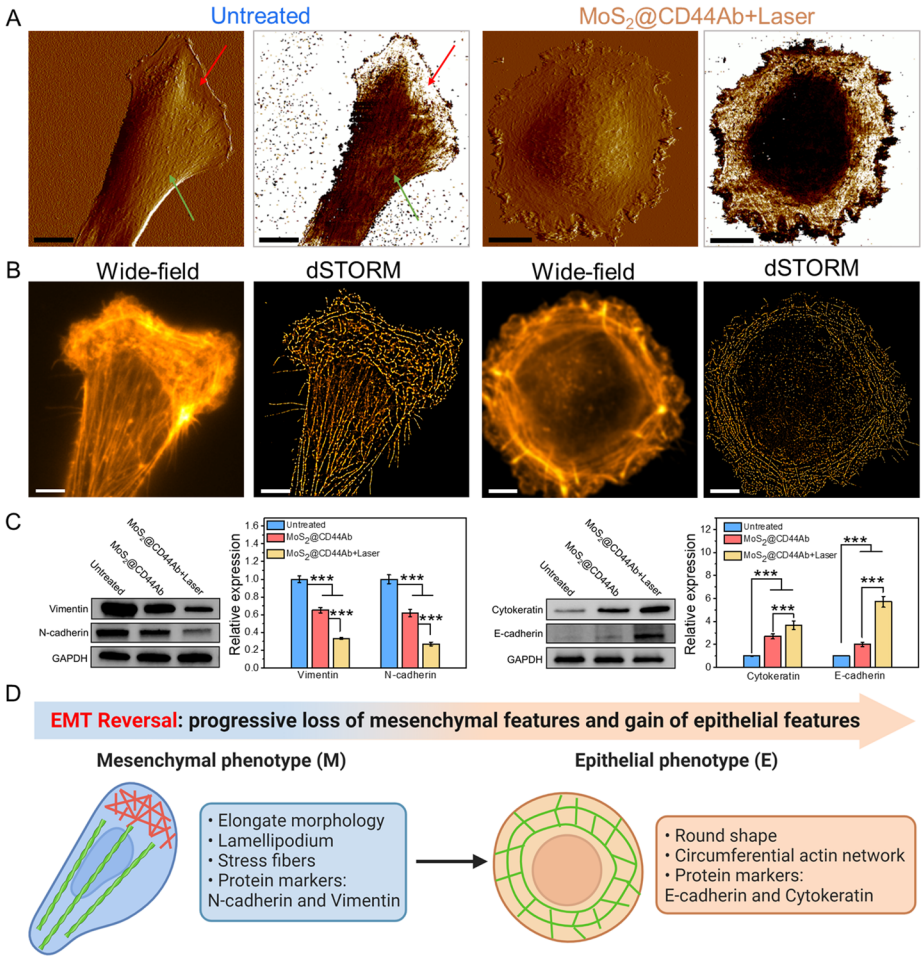

Figure 4. MoS_2@CD44Ab+Laser treatment mediates a phenotypic change of cancer cells. (A) Nanomechanical AFM imaging of untreated and MoS_2@CD44Ab+Laser-treated MDA-MB-231 cells. Correlated topography and modulus images are collected simultaneously. Live cells were probed by a spherical indenter, and the elastic modulus of each pixel was generated via fitting the corresponding force curve to a Hertz model. Green arrows mark the actin stress fibers, and red arrows point to the lamellipodium. Scale bars: 10 μm. (B) Wide-field and dSTORM images of single cells with and without MoS_2@CD44Ab+Laser treatment. dSTORM offers drastically improved imaging resolution by stochastically activating small numbers of fluorophores at a time. Scale bars: 5 μm. (C) Western blot analyses of EMT-related molecular markers. GAPDH was used as the housekeeping protein. Error bars: SD, $n = 3$. One-way ANOVA, $^{***}P < 0.001$. (D) Schematic summarizing the reversed EMT process in cancer cells.

by MoS_2@CD44Ab+Laser managed to invade across the Matrigel (a mimic for the extracellular matrix in a tumor microenvironment),[57,58] suggesting their significantly inhibited invasion ability. Reproducible results of migration/invasion assays are presented in Figures S11−S17. Together, these results demonstrate that MoS_2@CD44Ab and the moderate laser treatment synergistically and significantly inhibit the migration and invasion of MDA-MB-231 cells. We also tested the effect of these treatments on a CD44-overexpressed prostate cancer cell line, PC3-EMT (Figures S18 and S19). Similarly, our results showed that MoS_2@CD44Ab+Laser can stop the migration and invasion and attenuate the stemness and drug resistance of PC3-EMT cells, suggesting that this approach could be applicable to treat various cancers with high levels of CD44 biomarker.

Mounting evidence established a direct relation between the EMT and the stemness properties of cancer cells, both contribute to chemoresistance and metastasis.[59,60] The switch from epithelial to mesenchymal phenotype leads to high stemness of cancer cells, implying that EMT causes dedifferentiation.[61,62] In many cancers, the mesenchymal traits parallel the stemness-high cancer cells in which CD44 is highly expressed.[25] Therefore, we next determined to find whether MoS_2@CD44Ab+Laser treatment attenuates the stemness and promotes differentiation of MDA-MB-231 cells by altering the EMT process. We characterized the morphological change of single cells using nanomechanical AFM and direct stochastic optical reconstruction microscopy (dSTORM). Nanomechanical AFM measures the local elastic modulus of live cells to identify the actin filaments located in the top layer of cells.[63−65] Figure 4A shows the correlated surface topography and modulus images of single cells with or without MoS_2@CD44Ab+Laser treatment. Without treatment, MDA-MB-231 cells possessed an elongated cell shape with well-aligned actin stress fibers (green arrows) through the cell length and a lamellipodium (red arrows) on the leading edge of the cells; both are morphological characteristics of a mesenchymal phenotype.[66−68] In contrast, after treatment by MoS_2@CD44Ab+Laser, the cells noticeably transformed from an elongated shape into a cobblestone morphology (a typical feature of the epithelial phenotype),[69] accompanied by the loss of actin stress fibers and the gain of a thin peripheral

https://doi.org/10.1021/acs.nanolett.3c00089
Nano Lett. 2023, 23, 1989−1999

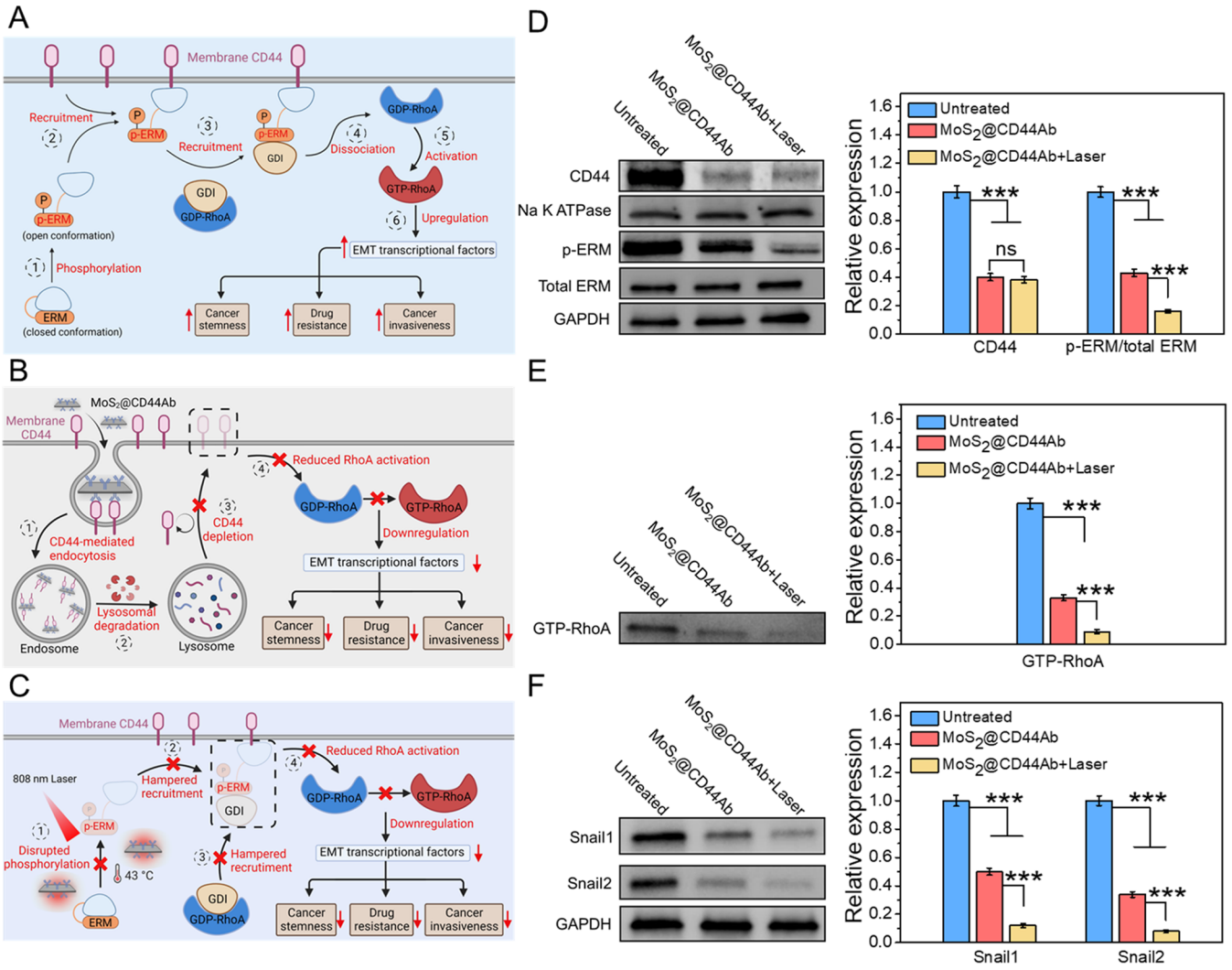

Figure 5. Molecular mechanism of reversed EMT and attenuated stemness. (A–C) Schematic illustrating the mechanism of how MoS_2@CD44Ab +Laser treatment affects the CD44-regulated EMT signaling pathway, thus causing the attenuation of stemness, drug resistance, and invasiveness. (D, E) Western blot quantification of membrane CD44, cytoplasmic p-ERM, total ERM, and GTP-RhoA in MDA-MB-231 cells after treatment by MoS_2@CD44Ab or MoS_2@CD44Ab+Laser. Na K ATPase and GAPDH serve as the housekeeping proteins for membrane protein and cytoplasmic protein, respectively. (F) Western blot analyses of Snail1 and Snail2 in MDA-MB-231 cells after treatment by MoS_2@CD44Ab or MoS_2@CD44Ab +Laser. Error bars: SD, $n = 3$. One-way ANOVA, $^{***}P < 0.001$, ns = no significant difference.

membrane. The aspect ratio of single cells reduced from 2.87 ± 0.21 to 1.22 ± 0.17 ($n = 10$) after the MoS_2@CD44Ab +Laser treatment. The average Young's modulus of the cellular body also decreased because of the loss of stress fibers (Figure S20). The morphological and cytoskeletal changes of MDA-MB-231 cells were further investigated using a super-resolution imaging tool, dSTORM.[70−72] Unlike AFM, dSTORM resolves the actin cytoskeleton in the bottom layer of cells using total internal reflection illumination. As shown in Figure 4B, the untreated cells presented typical mesenchymal traits, including an elongated cell shape, stress fibers parallel with the cell length, and an actin network within the lamellipodium, in accordance with our AFM observation. This also justifies the strong migratory/invasive propensity of MDA-MB-231 cells, which use lamellipodium to direct cell protrusion and stress fibers to generate contraction force to move the cell forward.[73] However, after treatment by MoS_2@CD44Ab+Laser, all the mesenchymal traits disappeared, including the loss of stress fibers and lamellipodium, and the cells shape became rounded with an actin network surrounding the full circumference (typical features of the epithelial phenotype).[74,75] Reproducible AFM and dSTORM results are presented in Figures S21−S24. Together, nanomechanical AFM and dSTORM highlight the morphological change of MDA-MB-231 cells after our treatment. Notably, the disappearance of mesenchymal traits along the gain of epithelial features are signatures of the reversed EMT process.

To further substantiate the cellular phenotypic change at the molecular level, we investigated EMT-related molecular markers using Western blotting (Figure 4C). The untreated cells expressed dominant levels of vimentin and N-cadherin, both known as mesenchymal markers.[76] On the other hand, the expressions of two corresponding epithelial markers, cytokeratin and E-cadherin, remained low in the untreated cells. However, the cells treated by MoS_2@CD44Ab alone showed an ∼40% decrease in both mesenchymal markers and ∼2-fold increase in both epithelial markers. More significantly, the cells treated by MoS_2@CD44Ab+Laser showed an ∼70% drop in both mesenchymal markers and 4−6-fold increase in both epithelial markers, suggesting a more complete transition

https://doi.org/10.1021/acs.nanolett.3c00089
Nano Lett. 2023, 23, 1989−1999

from a mesenchymal to an epithelial phenotype. Collectively, these data demonstrate that MoS_2@CD44Ab+Laser treatment attenuates the stemness of MDA-MB-231 cells by inducing a reversed EMT process and converting the cells from a mesenchymal to an epithelial phenotype (Figure 4D). Considering EMT in cancer has been depicted as a dedifferentiation event (increasing stemness),[62] the reversed EMT here suggests a differentiation process (attenuation of stemness) of the cancer cells.

So far, we have demonstrated that MoS_2@CD44Ab+Laser treatment attenuates the stemness of cancer cells via reversing the EMT process, while the molecular mechanism by which MoS_2@CD44Ab+Laser reverses the EMT remained undefined. Therefore, we finally examined how MoS_2@CD44Ab +Laser treatment reversed EMT and thus attenuated stemness at the molecular level. Previous research established the functional roles of CD44 in the regulation of the EMT-related signaling pathway.[77−79] As illustrated in Figure 5A, transmembrane CD44 first recruits phosphorylated ezrin/radixin/moesin (p-ERM) from the cytosol to form a CD44-p-ERM complex, which further recruits Rho guanine nucleotide dissociation inhibitor alpha (RhoGDIα, an endogenous inhibitor for RhoA), promoting the release of GDP-RhoA (inactive form of RhoA) for the subsequent activation to GTP-RhoA. The upregulation of GTP-RhoA (active form of RhoA) mediates the EMT process by upregulating EMT transcriptional factors such as Snail1 and Snail2, favoring cancer stemness, migration/invasion, and drug resistance.[76] Based on these findings and our earlier results, we proposed to test the following hypothesis: CD44-targeted MoS_2 nanosheets and the moderate photothermal effect can deplete membrane CD44 and impede ERM phosphorylation, respectively, where both factors would synergistically contribute to the downregulation of RhoA activation, leading to the reversed EMT and attenuated cancer stemness (Figure 5B,C).

Western blotting was used to quantify the molecular markers along the CD44-regulated EMT signaling pathway. Figure 5D shows that the amount of membrane CD44 decreased by ∼60% for both MoS_2@CD44Ab- and MoS_2@CD44Ab+Laser-treated MDA-MB-231 cells. As illustrated in Figure 5B, the downregulation of membrane CD44 can be attributed to the cell uptake of CD44-targeted MoS_2, depleting membrane CD44 into lysosomal degradative compartments, which is supported by our FITC/Lysotracker colocalization assay. For the cells treated by MoS_2@CD44Ab alone, the downregulation of membrane CD44 consistently led to a ∼60% reduction of ERM phosphorylation (p-ERM) and RhoA activation (GTP-RhoA), due to the indispensable role of CD44 in the regulation of ERM phosphorylation (Figure 5D,E).[80] As anticipated, the downstream EMT transcriptional factors (i.e., Snail1, Snail2) showed a 50−60% decrease (Figure 5F), which explains our earlier results that MoS_2@CD44Ab alone partially suppressed mammosphere formation, expressions of stemness and mesenchymal markers, and migration/invasion of cancer cells. This is also in agreement with previous reports suggesting that knock-down of CD44 partially converts the cells from a mesenchymal to an epithelial phenotype.[26,56] Notably, in the cells treated by MoS_2@CD44Ab+Laser, both p-ERM and GTP-RhoA levels showed a larger decrease (by ∼80−90%) compared to those cells treated by MoS_2@CD44Ab alone (only by ∼60%), which implied the additional impact of photothermal treatment on the ERM phosphorylation (Figure 5D,E). This is reasonable considering the disruptive effect of elevated temperature on the intracellular protein phosphorylation as reported previously in a variety of cell types.[81−83] Herein, we reason that the increase of intracellular temperature induced by the photothermal effect of cell-internalized MoS_2@CD44Ab could disrupt the ERM phosphorylation, thus impeding the activation of GDP-RhoA to GTP-RhoA (as illustrated by Figure 5C). As a result, the downstream EMT transcriptional factors (i.e., Snail1, Snail2) showed a consistent ∼90% decrease (Figure 5F). The decrease in EMT transcriptional factors has been shown to drive cancer cells from a mesenchymal to an epithelial state, along with stemness attenuation.[84−86] Together, these results reveal a molecular mechanism by which MoS_2@CD44Ab and laser treatment reverse the EMT process in a sequential and synergistic manner: First, cell uptake of MoS_2@CD44Ab depletes the membrane CD44 and reduces the formation of CD44-p-ERM complex to recruit RhoA inhibitor (RhoGDIα), leading to the downregulated RhoA activation. Subsequently, the moderate photothermal effect disrupts the phosphorylation of ERM and thus decreases the availability of p-ERM for the formation of CD44-p-ERM complex, further hampering the RhoGDIα recruitment and RhoA activation. Such a collective negative effect on the RhoA activation results in the downregulation in EMT transcriptional factors, leading to a reversed EMT process.

In summary, we have demonstrated a "photothermal differentiation" approach to induce the differentiation of cancer stem cells, leading to attenuation of cancer cell stemness, chemoresistance, and metastasis. After treatment by CD44-targeted MoS_2 nanosheets and a moderate photothermal effect, CD44-overexpressed, high-stemness breast and prostate cancer cells exhibited attenuated mammosphere-forming ability, improved response to a chemotherapeutic drug (doxorubicin), and inhibited migration and invasion. The attenuation of cancer cell stemness was in parallel with a cellular change from a mesenchymal to an epithelial phenotype, suggesting that a reversed EMT process was induced by the treatment. Further molecular studies revealed the mechanism by which this approach effectively modulated the CD44-regulated EMT signaling pathway, causing a reversed EMT process and attenuated stemness in cancer cells. Overall, this work presents a unique concept, via the use of rationally designed nanomaterials, to address cancer stemness-associated challenges. From a clinical perspective, this approach could be applicable to treat multiple cancers due to the high levels of the CD44 biomarker on various cancers. This method holds great potential in complementing conventional surgical resection and chemotherapy, where pretreating tumors with this approach could impede cancer cell migration and make refractory cancer cells more sensitive to anticancer drugs, thereby increasing the effectiveness of surgical resection and chemotherapy and minimizing the likelihood of metastasis and relapse.

■ ASSOCIATED CONTENT

Supporting Information

The Supporting Information is available free of charge at https://pubs.acs.org/doi/10.1021/acs.nanolett.3c00089.

Experimental section, list of antibodies, TEM images of MoS_2@PA@CD44Ab and bare MoS_2, hydrodynamic size and UV−vis spectra of MoS_2@PA@CD44Ab, immunofluorescence staining of surface CD44, cellular

https://doi.org/10.1021/acs.nanolett.3c00089
Nano Lett. 2023, 23, 1989−1999

uptake and intracellular localization of MoS_2, live and dead staining assay, mammosphere formation assay, wound-healing and transwell invasion assays, Young's modulus of single cells, and AFM and dSTORM images of single cells, uncropped Western blot images (PDF)

AUTHOR INFORMATION

Corresponding Author

Congzhou Wang − *Nanoscience and Biomedical Engineering, South Dakota School of Mines and Technology, Rapid City, South Dakota 57701, United States; BioSystems Networks & Translational Research (BioSNTR), Rapid City, South Dakota 57701, United States;* orcid.org/0000-0001-6132-447X; Email: congzhou.wang@sdsmt.edu

Authors

Jinyuan Liu − *Nanoscience and Biomedical Engineering, South Dakota School of Mines and Technology, Rapid City, South Dakota 57701, United States; BioSystems Networks & Translational Research (BioSNTR), Rapid City, South Dakota 57701, United States*

Steve Smith − *Nanoscience and Biomedical Engineering, South Dakota School of Mines and Technology, Rapid City, South Dakota 57701, United States; BioSystems Networks & Translational Research (BioSNTR), Rapid City, South Dakota 57701, United States*

Complete contact information is available at: https://pubs.acs.org/10.1021/acs.nanolett.3c00089

Notes

The authors declare no competing financial interest.

ACKNOWLEDGMENTS

The authors acknowledge support from a National Science Foundation CAREER Award (2143972) and the National Institutes of Health through Award R15CA274349.

REFERENCES

(1) Clevers, H. The cancer stem cell: premises, promises and challenges. *Nature medicine* **2011**, *17* (3), 313−9.

(2) Nguyen, D. X.; Bos, P. D.; Massagué, J. Metastasis: from dissemination to organ-specific colonization. *Nature reviews. Cancer* **2009**, *9* (4), 274−84.

(3) Meacham, C. E.; Morrison, S. J. Tumour heterogeneity and cancer cell plasticity. *Nature* **2013**, *501* (7467), 328−37.

(4) Batlle, E.; Clevers, H. Cancer stem cells revisited. *Nature medicine* **2017**, *23* (10), 1124−1134.

(5) Gupta, P. B.; Onder, T. T.; Jiang, G.; Tao, K.; Kuperwasser, C.; Weinberg, R. A.; Lander, E. S. Identification of Selective Inhibitors of Cancer Stem Cells by High-Throughput Screening. *Cell* **2009**, *138* (4), 645−659.

(6) Yin, F.; Gu, B.; Li, J.; Panwar, N.; Liu, Y.; Li, Z.; Yong, K.-T.; Tang, B. Z. In vitro anticancer activity of AIEgens. *Biomaterials Science* **2019**, *7* (9), 3855−3865.

(7) Pattabiraman, D. R.; Weinberg, R. A. Tackling the cancer stem cells - what challenges do they pose? *Nature reviews. Drug discovery* **2014**, *13* (7), 497−512.

(8) Chaffer, C. L.; Brueckmann, I.; Scheel, C.; Kaestli, A. J.; Wiggins, P. A.; Rodrigues, L. O.; Brooks, M.; Reinhardt, F.; Su, Y.; Polyak, K.; Arendt, L. M.; Kuperwasser, C.; Bierie, B.; Weinberg, R. A. Normal and neoplastic nonstem cells can spontaneously convert to a stem-like state. *Proc. Natl. Acad. Sci. U.S.A.* **2011**, *108* (19), 7950−5.

(9) Yang, G.; Quan, Y.; Wang, W.; Fu, Q.; Wu, J.; Mei, T.; Li, J.; Tang, Y.; Luo, C.; Ouyang, Q.; Chen, S.; Wu, L.; Hei, T. K.; Wang, Y. Dynamic equilibrium between cancer stem cells and non-stem cancer cells in human SW620 and MCF-7 cancer cell populations. *British journal of cancer* **2012**, *106* (9), 1512−9.

(10) Yu, Y.; Yang, X.; Reghu, S.; Kaul, S. C.; Wadhwa, R.; Miyako, E. Photothermogenetic inhibition of cancer stemness by near-infrared-light-activatable nanocomplexes. *Nat. Commun.* **2020**, *11* (1), 4117.

(11) Pattabiraman, D. R.; Bierie, B.; Kober, K. I.; Thiru, P.; Krall, J. A.; Zill, C.; Reinhardt, F.; Tam, W. L.; Weinberg, R. A. Activation of PKA leads to mesenchymal-to-epithelial transition and loss of tumor-initiating ability. *Science* **2016**, *351* (6277), aad3680.

(12) Pan, Y.; Ma, X.; Liu, C.; Xing, J.; Zhou, S.; Parshad, B.; Schwerdtle, T.; Li, W.; Wu, A.; Haag, R. Retinoic Acid-Loaded Dendritic Polyglycerol-Conjugated Gold Nanostars for Targeted Photothermal Therapy in Breast Cancer Stem Cells. *ACS Nano* **2021**, *15* (9), 15069−15084.

(13) Shen, S.; Xu, X.; Lin, S.; Zhang, Y.; Liu, H.; Zhang, C.; Mo, R. A nanotherapeutic strategy to overcome chemotherapeutic resistance of cancer stem-like cells. *Nat. Nanotechnol.* **2021**, *16* (1), 104−113.

(14) Sun, R.; Liu, Y.; Li, S. Y.; Shen, S.; Du, X. J.; Xu, C. F.; Cao, Z. T.; Bao, Y.; Zhu, Y. H.; Li, Y. P.; Yang, X. Z.; Wang, J. Co-delivery of all-trans-retinoic acid and doxorubicin for cancer therapy with synergistic inhibition of cancer stem cells. *Biomaterials* **2015**, *37*, 405−14.

(15) Li, R. J.; Ying, X.; Zhang, Y.; Ju, R. J.; Wang, X. X.; Yao, H. J.; Men, Y.; Tian, W.; Yu, Y.; Zhang, L.; Huang, R. J.; Lu, W. L. All-trans retinoic acid stealth liposomes prevent the relapse of breast cancer arising from the cancer stem cells. *Journal of controlled release: official journal of the Controlled Release Society* **2011**, *149* (3), 281−91.

(16) Ferreira, R.; Napoli, J.; Enver, T.; Bernardino, L.; Ferreira, L. Advances and challenges in retinoid delivery systems in regenerative and therapeutic medicine. *Nat. Commun.* **2020**, *11* (1), 4265.

(17) Chen, C.; Zhao, S.; Karnad, A.; Freeman, J. W. The biology and role of CD44 in cancer progression: therapeutic implications. *J. Hematol Oncol* **2018**, *11* (1), 64.

(18) Al-Othman, N.; Alhendi, A.; Ihbaisha, M.; Barahmeh, M.; Alqaraleh, M.; Al-Momany, B. Z. Role of CD44 in breast cancer. *Breast disease* **2020**, *39* (1), 1−13.

(19) Iczkowski, K. A. Cell adhesion molecule CD44: its functional roles in prostate cancer. *Am. J. Transl Res.* **2010**, *3* (1), 1−7.

(20) Bhattacharya, R.; Mitra, T.; Ray Chaudhuri, S.; Roy, S. S. Mesenchymal splice isoform of CD44 (CD44s) promotes EMT/invasion and imparts stem-like properties to ovarian cancer cells. *Journal of Cellular Biochemistry* **2018**, *119* (4), 3373−3383.

(21) Zhao, S.; Chen, C.; Chang, K.; Karnad, A.; Jagirdar, J.; Kumar, A. P.; Freeman, J. W. CD44 Expression Level and Isoform Contributes to Pancreatic Cancer Cell Plasticity, Invasiveness, and Response to Therapy. *Clinical cancer research: an official journal of the American Association for Cancer Research* **2016**, *22* (22), 5592−5604.

(22) Cho, S. H.; Park, Y. S.; Kim, H. J.; Kim, C. H.; Lim, S. W.; Huh, J. W.; Lee, J. H.; Kim, H. R. CD44 enhances the epithelial-mesenchymal transition in association with colon cancer invasion. *International journal of oncology* **2012**, *41* (1), 211−8.

(23) Zhang, J.; He, X.; Wan, Y.; Zhang, H.; Tang, T.; Zhang, M.; Yu, S.; Zhao, W.; Chen, L. CD44 promotes hepatocellular carcinoma progression via upregulation of YAP. *Experimental Hematology & Oncology* **2021**, *10* (1), 54.

(24) Thapa, R.; Wilson, G. D. The Importance of CD44 as a Stem Cell Biomarker and Therapeutic Target in Cancer. *Stem Cells Int.* **2016**, *2016*, 2087204.

(25) Xu, H.; Tian, Y.; Yuan, X.; Wu, H.; Liu, Q.; Pestell, R. G.; Wu, K. The role of CD44 in epithelial-mesenchymal transition and cancer development. *Onco Targets Ther* **2015**, *8*, 3783−92.

(26) Gao, Y.; Ruan, B.; Liu, W.; Wang, J.; Yang, X.; Zhang, Z.; Li, X.; Duan, J.; Zhang, F.; Ding, R.; Tao, K.; Dou, K. Knockdown of CD44 inhibits the invasion and metastasis of hepatocellular carcinoma both in vitro and in vivo by reversing epithelial-mesenchymal transition. *Oncotarget* **2015**, *6* (10), 7828−7837.

(27) Singh, A.; Settleman, J. EMT, cancer stem cells and drug resistance: an emerging axis of evil in the war on cancer. *Oncogene* **2010**, *29* (34), 4741−51.

(28) Xu, H.; Niu, M.; Yuan, X.; Wu, K.; Liu, A. CD44 as a tumor biomarker and therapeutic target. *Experimental Hematology & Oncology* **2020**, *9* (1), 36.
(29) Yan, Y.; Zuo, X.; Wei, D. Concise Review: Emerging Role of CD44 in Cancer Stem Cells: A Promising Biomarker and Therapeutic Target. *Stem Cells Translational Medicine* **2015**, *4* (9), 1033−1043.
(30) Zhang, M.; Wang, W.; Mohammadniaei, M.; Zheng, T.; Zhang, Q.; Ashley, J.; Liu, S.; Sun, Y.; Tang, B. Z. Upregulating Aggregation-Induced-Emission Nanoparticles with Blood−Tumor-Barrier Permeability for Precise Photothermal Eradication of Brain Tumors and Induction of Local Immune Responses. *Adv. Mater.* **2021**, *33* (22), 2008802.
(31) Song, N.; Zhang, Z.; Liu, P.; Dai, D.; Chen, C.; Li, Y.; Wang, L.; Han, T.; Yang, Y.-W.; Wang, D.; Tang, B. Z. Pillar[5]arene-Modified Gold Nanorods as Nanocarriers for Multi-Modal Imaging-Guided Synergistic Photodynamic-Photothermal Therapy. *Adv. Funct. Mater.* **2021**, *31* (21), 2009924.
(32) Wang, H.; Chang, J.; Shi, M.; Pan, W.; Li, N.; Tang, B. A Dual-Targeted Organic Photothermal Agent for Enhanced Photothermal Therapy. *Angew. Chem., Int. Ed.* **2019**, *58* (4), 1057−1061.
(33) Li, N.; Sun, Q.; Yu, Z.; Gao, X.; Pan, W.; Wan, X.; Tang, B. Nuclear-Targeted Photothermal Therapy Prevents Cancer Recurrence with Near-Infrared Triggered Copper Sulfide Nanoparticles. *ACS Nano* **2018**, *12* (6), 5197−5206.
(34) Shi, M.; Fu, Z.; Pan, W.; Chen, Y.; Wang, K.; Zhou, P.; Li, N.; Tang, B. A Protein-Binding Molecular Photothermal Agent for Tumor Ablation. *Angew. Chem., Int. Ed.* **2021**, *60* (24), 13564−13568.
(35) Wang, W.; Wu, F.; Mohammadniaei, M.; Zhang, M.; Li, Y.; Sun, Y.; Tang, B. Z. Genetically edited T-cell membrane coated AIEgen nanoparticles effectively prevents glioblastoma recurrence. *Biomaterials* **2023**, *293*, 121981.
(36) Seth, A.; Gholami Derami, H.; Gupta, P.; Wang, Z.; Rathi, P.; Gupta, R.; Cao, T.; Morrissey, J. J.; Singamaneni, S. Polydopamine−Mesoporous Silica Core−Shell Nanoparticles for Combined Photothermal Immunotherapy. *ACS Appl. Mater. Interfaces* **2020**, *12* (38), 42499−42510.
(37) Younis, M. R.; Wang, C.; An, R.; Wang, S.; Younis, M. A.; Li, Z.-Q.; Wang, Y.; Ihsan, A.; Ye, D.; Xia, X.-H. Low Power Single Laser Activated Synergistic Cancer Phototherapy Using Photosensitizer Functionalized Dual Plasmonic Photothermal Nanoagents. *ACS Nano* **2019**, *13* (2), 2544−2557.
(38) Zhu, X.; Ji, X.; Kong, N.; Chen, Y.; Mahmoudi, M.; Xu, X.; Ding, L.; Tao, W.; Cai, T.; Li, Y.; Gan, T.; Barrett, A.; Bharwani, Z.; Chen, H.; Farokhzad, O. C. Intracellular Mechanistic Understanding of 2D MoS2 Nanosheets for Anti-Exocytosis-Enhanced Synergistic Cancer Therapy. *ACS Nano* **2018**, *12* (3), 2922−2938.
(39) Liu, T.; Wang, C.; Gu, X.; Gong, H.; Cheng, L.; Shi, X.; Feng, L.; Sun, B.; Liu, Z. Drug Delivery with PEGylated MoS2 Nano-sheets for Combined Photothermal and Chemotherapy of Cancer. *Adv. Mater.* **2014**, *26* (21), 3433−3440.
(40) Hu, W.; Xiao, T.; Li, D.; Fan, Y.; Xing, L.; Wang, X.; Li, Y.; Shi, X.; Shen, M. Intelligent Molybdenum Disulfide Complexes as a Platform for Cooperative Imaging-Guided Tri-Mode Chemo-Photothermo-Immunotherapy. *Advanced Science* **2021**, *8* (14), 2100165.
(41) Kong, L.; Xing, L.; Zhou, B.; Du, L.; Shi, X. Dendrimer-Modified MoS2 Nanoflakes as a Platform for Combinational Gene Silencing and Photothermal Therapy of Tumors. *ACS Appl. Mater. Interfaces* **2017**, *9* (19), 15995−16005.
(42) Liu, Y.; Chen, C.; Qian, P.; Lu, X.; Sun, B.; Zhang, X.; Wang, L.; Gao, X.; Li, H.; Chen, Z.; Tang, J.; Zhang, W.; Dong, J.; Bai, R.; Lobie, P. E.; Wu, Q.; Liu, S.; Zhang, H.; Zhao, F.; Wicha, M. S.; Zhu, T.; Zhao, Y. Gd-metallofullerenol nanomaterial as non-toxic breast cancer stem cell-specific inhibitor. *Nat. Commun.* **2015**, *6* (1), 5988.
(43) Omara-Opyene, A. L.; Qiu, J.; Shah, G. V.; Iczkowski, K. A. Prostate cancer invasion is influenced more by expression of a CD44 isoform including variant 9 than by Muc18. *Laboratory investigation; a journal of technical methods and pathology* **2004**, *84* (7), 894−907.
(44) Coleman, J. N.; Lotya, M.; O'Neill, A.; Bergin, S. D.; King, P. J.; Khan, U.; Young, K.; Gaucher, A.; De, S.; Smith, R. J.; Shvets, I. V.; Arora, S. K.; Stanton, G.; Kim, H.-Y.; Lee, K.; Kim, G. T.; Duesberg, G. S.; Hallam, T.; Boland, J. J.; Wang, J. J.; Donegan, J. F.; Grunlan, J. C.; Moriarty, G.; Shmeliov, A.; Nicholls, R. J.; Perkins, J. M.; Grieveson, E. M.; Theuwissen, K.; McComb, D. W.; Nellist, P. D.; Nicolosi, V. Two-Dimensional Nanosheets Produced by Liquid Exfoliation of Layered Materials. *Science* **2011**, *331* (6017), 568−571.
(45) Guan, G.; Zhang, S.; Liu, S.; Cai, Y.; Low, M.; Teng, C. P.; Phang, I. Y.; Cheng, Y.; Duei, K. L.; Srinivasan, B. M.; Zheng, Y.; Zhang, Y.-W.; Han, M.-Y. Protein Induces Layer-by-Layer Exfoliation of Transition Metal Dichalcogenides. *J. Am. Chem. Soc.* **2015**, *137* (19), 6152−6155.
(46) Kolesnikova, T. A.; Kiragosyan, G.; Le, T. H. N.; Springer, S.; Winterhalter, M. Protein A Functionalized Polyelectrolyte Microcapsules as a Universal Platform for Enhanced Targeting of Cell Surface Receptors. *ACS Appl. Mater. Interfaces* **2017**, *9* (13), 11506−11517.
(47) Sivaram, A. J.; Wardiana, A.; Alcantara, S.; Sonderegger, S. E.; Fletcher, N. L.; Houston, Z. H.; Howard, C. B.; Mahler, S. M.; Alexander, C.; Kent, S. J.; Bell, C. A.; Thurecht, K. J. Controlling the Biological Fate of Micellar Nanoparticles: Balancing Stealth and Targeting. *ACS Nano* **2020**, *14* (10), 13739−13753.
(48) Sheridan, C.; Kishimoto, H.; Fuchs, R. K.; Mehrotra, S.; Bhat-Nakshatri, P.; Turner, C. H.; Goulet, R., Jr; Badve, S.; Nakshatri, H. CD44+/CD24- breast cancer cells exhibit enhanced invasive properties: an early step necessary for metastasis. *Breast cancer research: BCR* **2006**, *8* (5), R59.
(49) Xu, Y.; Wang, J.; Li, X.; Liu, Y.; Dai, L.; Wu, X.; Chen, C. Selective inhibition of breast cancer stem cells by gold nanorods mediated plasmonic hyperthermia. *Biomaterials* **2014**, *35* (16), 4667−77.
(50) Wang, H.; Agarwal, P.; Zhao, S.; Yu, J.; Lu, X.; He, X. Combined cancer therapy with hyaluronan-decorated fullerene-silica multifunctional nanoparticles to target cancer stem-like cells. *Biomaterials* **2016**, *97*, 62−73.
(51) Paholak, H. J.; Stevers, N. O.; Chen, H.; Burnett, J. P.; He, M.; Korkaya, H.; McDermott, S. P.; Deol, Y.; Clouthier, S. G.; Luther, T.; Li, Q.; Wicha, M. S.; Sun, D. Elimination of epithelial-like and mesenchymal-like breast cancer stem cells to inhibit metastasis following nanoparticle-mediated photothermal therapy. *Biomaterials* **2016**, *104*, 145−57.
(52) Phi, L. T. H.; Sari, I. N.; Yang, Y.-G.; Lee, S.-H.; Jun, N.; Kim, K. S.; Lee, Y. K.; Kwon, H. Y. Cancer Stem Cells (CSCs) in Drug Resistance and their Therapeutic Implications in Cancer Treatment. *Stem Cells Int.* **2018**, *2018*, 5416923.
(53) Li, Y.; Wang, Z.; Ajani, J. A.; Song, S. Drug resistance and Cancer stem cells. *Cell Communication and Signaling* **2021**, *19* (1), 19.
(54) Gooding, A. J.; Schiemann, W. P. Epithelial-Mesenchymal Transition Programs and Cancer Stem Cell Phenotypes: Mediators of Breast Cancer Therapy Resistance. *Molecular cancer research: MCR* **2020**, *18* (9), 1257−1270.
(55) Nam, K.; Oh, S.; Lee, K. M.; Yoo, S. A.; Shin, I. CD44 regulates cell proliferation, migration, and invasion via modulation of c-Src transcription in human breast cancer cells. *Cellular signalling* **2015**, *27* (9), 1882−94.
(56) Kong, L.; Ji, H.; Gan, X.; Cao, S.; Li, Z.; Jin, Y. Knockdown of CD44 inhibits proliferation, migration and invasion of osteosarcoma cells accompanied by downregulation of cathepsin S. *Journal of Orthopaedic Surgery and Research* **2022**, *17* (1), 154.
(57) He, X.; Yang, Y.; Li, L.; Zhang, P.; Guo, H.; Liu, N.; Yang, X.; Xu, F. Engineering extracellular matrix to improve drug delivery for cancer therapy. *Drug Discovery Today* **2020**, *25* (9), 1727−1734.
(58) Guo, H.; Zhang, T.; Yu, Y.; Xu, F. Cancer Physical Hallmarks as New Targets for Improved Immunotherapy. *Trends in Cell Biology* **2021**, *31* (7), 520−524.
(59) Wang, S.-S.; Jiang, J.; Liang, X.-H.; Tang, Y.-L. Links between cancer stem cells and epithelial-mesenchymal transition. *Onco Targets Ther* **2015**, *8*, 2973−2980.

https://doi.org/10.1021/acs.nanolett.3c00089
Nano Lett. 2023, 23, 1989−1999

(60) Tanabe, S.; Quader, S.; Cabral, H.; Ono, R. Interplay of EMT and CSC in Cancer and the Potential Therapeutic Strategies. *Frontiers in pharmacology* **2020**, *11*, 904.
(61) May, C. D.; Sphyris, N.; Evans, K. W.; Werden, S. J.; Guo, W.; Mani, S. A. Epithelial-mesenchymal transition and cancer stem cells: a dangerously dynamic duo in breast cancer progression. *Breast cancer research: BCR* **2011**, *13* (1), 202.
(62) Wang, H.; Unternaehrer, J. J. Epithelial-mesenchymal Transition and Cancer Stem Cells: At the Crossroads of Differentiation and Dedifferentiation. *Developmental dynamics: an official publication of the American Association of Anatomists* **2019**, *248* (1), 10−20.
(63) Dumitru, A. C.; Poncin, M. A.; Conrard, L.; Dufrêne, Y. F.; Tyteca, D.; Alsteens, D. Nanoscale membrane architecture of healthy and pathological red blood cells. *Nanoscale Horizons* **2018**, *3* (3), 293−304.
(64) Eghiaian, F.; Rigato, A.; Scheuring, S. Structural, mechanical, and dynamical variability of the actin cortex in living cells. *Biophysical journal* **2015**, *108* (6), 1330−1340.
(65) Calzado-Martín, A.; Encinar, M.; Tamayo, J.; Calleja, M.; San Paulo, A. Effect of Actin Organization on the Stiffness of Living Breast Cancer Cells Revealed by Peak-Force Modulation Atomic Force Microscopy. *ACS Nano* **2016**, *10* (3), 3365−3374.
(66) Wang, M.; Cheng, B.; Yang, Y.; Liu, H.; Huang, G.; Han, L.; Li, F.; Xu, F. Microchannel Stiffness and Confinement Jointly Induce the Mesenchymal-Amoeboid Transition of Cancer Cell Migration. *Nano Lett.* **2019**, *19* (9), 5949−5958.
(67) Huang, G.; Xu, F.; Genin, G. M.; Lu, T. J. Mechanical microenvironments of living cells: a critical frontier in mechanobiology. *Acta Mechanica Sinica* **2019**, *35* (2), 265−269.
(68) Vallenius, T. Actin stress fibre subtypes in mesenchymal-migrating cells. *Open Biology* **2013**, *3* (6), 130001.
(69) Voutsadakis, I. A. Epithelial-Mesenchymal Transition (EMT) and Regulation of EMT Factors by Steroid Nuclear Receptors in Breast Cancer: A Review and in Silico Investigation. *Journal of Clinical Medicine* **2016**, *5* (1), 11.
(70) van de Linde, S.; Löschberger, A.; Klein, T.; Heidbreder, M.; Wolter, S.; Heilemann, M.; Sauer, M. Direct stochastic optical reconstruction microscopy with standard fluorescent probes. *Nat. Protoc.* **2011**, *6* (7), 991−1009.
(71) Dempsey, G. T.; Vaughan, J. C.; Chen, K. H.; Bates, M.; Zhuang, X. Evaluation of fluorophores for optimal performance in localization-based super-resolution imaging. *Nat. Methods* **2011**, *8* (12), 1027−1036.
(72) Xu, J.; Ma, H.; Liu, Y. Stochastic Optical Reconstruction Microscopy (STORM). *Current Protocols in Cytometry* **2017**, *81* (1), 12.46.1−12.46.27.
(73) Innocenti, M. New insights into the formation and the function of lamellipodia and ruffles in mesenchymal cell migration. *Cell Adh Migr* **2018**, *12* (5), 401−416.
(74) Furukawa, K. T.; Yamashita, K.; Sakurai, N.; Ohno, S. The Epithelial Circumferential Actin Belt Regulates YAP/TAZ through Nucleocytoplasmic Shuttling of Merlin. *Cell Reports* **2017**, *20* (6), 1435−1447.
(75) Bosch-Fortea, M.; Martín-Belmonte, F. Mechanosensitive adhesion complexes in epithelial architecture and cancer onset. *Curr. Opin. Cell Biol.* **2018**, *50*, 42−49.
(76) Zeng, Q.; Li, W.; Lu, D.; Wu, Z.; Duan, H.; Luo, Y.; Feng, J.; Yang, D.; Fu, L.; Yan, X. CD146, an epithelial-mesenchymal transition inducer, is associated with triple-negative breast cancer. *Proc. Natl. Acad. Sci. U. S. A.* **2012**, *109* (4), 1127−1132.
(77) Takahashi, K.; Sasaki, T.; Mammoto, A.; Takaishi, K.; Kameyama, T.; Tsukita, S.; Takai, Y.; et al. Direct interaction of the Rho GDP dissociation inhibitor with ezrin/radixin/moesin initiates the activation of the Rho small G protein. *J. Biol. Chem.* **1997**, *272* (37), 23371−5.
(78) Dovas, A.; Couchman, J. R. RhoGDI: multiple functions in the regulation of Rho family GTPase activities. *Biochemical journal* **2005**, *390* (1), 1−9.
(79) Hirao, M.; Sato, N.; Kondo, T.; Yonemura, S.; Monden, M.; Sasaki, T.; Takai, Y.; Tsukita, S.; Tsukita, S. Regulation mechanism of ERM (ezrin/radixin/moesin) protein/plasma membrane association: possible involvement of phosphatidylinositol turnover and Rho-dependent signaling pathway. *J. Cell Biol.* **1996**, *135* (1), 37−51.
(80) Thorne, R. F.; Legg, J. W.; Isacke, C. M. The role of the CD44 transmembrane and cytoplasmic domains in co-ordinating adhesive and signalling events. *Journal of Cell Science* **2004**, *117* (3), 373−380.
(81) Wu, Y.; Ali, M. R. K.; Dong, B.; Han, T.; Chen, K.; Chen, J.; Tang, Y.; Fang, N.; Wang, F.; El-Sayed, M. A. Gold Nanorod Photothermal Therapy Alters Cell Junctions and Actin Network in Inhibiting Cancer Cell Collective Migration. *ACS Nano* **2018**, *12* (9), 9279−9290.
(82) Dharmasiri, S.; Harrington, H. M.; Dharmasiri, N. Heat shock modulates phosphorylation status and activity of nucleoside diphosphate kinase in cultured sugarcane cells. *Plant Cell Reports* **2010**, *29* (11), 1305−1314.
(83) Duncan, R. F.; Hershey, J. W. Protein synthesis and protein phosphorylation during heat stress, recovery, and adaptation. *J. Cell Biol.* **1989**, *109* (4), 1467−1481.
(84) Wang, Y.; Shi, J.; Chai, K.; Ying, X.; Zhou, B. P. The Role of Snail in EMT and Tumorigenesis. *Curr. Cancer Drug Targets* **2013**, *13* (9), 963−972.
(85) Wang, Z.; Xia, F.; Labib, M.; Ahmadi, M.; Chen, H.; Das, J.; Ahmed, S. U.; Angers, S.; Sargent, E. H.; Kelley, S. O. Nanostructured Architectures Promote the Mesenchymal−Epithelial Transition for Invasive Cells. *ACS Nano* **2020**, *14* (5), 5324−5336.
(86) Alves, C. C.; Carneiro, F.; Hoefler, H.; Becker, K.-F. Role of the epithelial-mesenchymal transition regulator Slug in primary human cancers. *FBL* **2009**, *14* (8), 3035−3050.

https://doi.org/10.1021/acs.nanolett.3c00089
Nano Lett. 2023, 23, 1989−1999